

## RESERVOIR CHARACTERIZATION USING CORE DATA AND WELL LOGGING ANALYSIS IN OBAYIED FIELD, WESTERN DESERT, EGYPT

A.N.A. GOMAA, A.M. EL-SAYED and N.M.H. ABU ASHOUR

Geophysics Department, Faculty of Science, Ain Shams University.

توصيف الخزان البترولي باستخدام بيانات تحاليل العينات اللبية وتسجيلات الآبار  
في حقل الأبيض بالصحراء الغربية، مصر

**الخلاصة:** تم استخدام تسجيلات آبار متنوعة لعدد ٥ آبار وبيانات المسامية اللبية للآبار (Well-1, Well-4, Well-3) بمنطقة حقل الأبيض بالصحراء الغربية في دراسة الخصائص الصخرية والبتروفيزيائية لخزانات Upper & Lower Safa Members وحساب متوسط الخصائص الصخرية والبتروفيزيائية لها، وبواسطة تحليل بيانات المسامية والمقاومة الكهربائية للنطاقات الخازنة للمواد الهيدروكربونية ذات النفاذية تم تحديد طبيعة السوائل المتواجدة بها. كما أن فهم التغيرات التي تحدث في قياسات المقاومة الكهربائية خلال المناطق الغربية من تجويف البئر عند المناطق ذات النفاذية تساعد على تفسير قياسات أدوات قياس المقاومة الكهربائية للنطاقات المشبعة بالمواد الهيدروكربونية والمياه. كما تظهر قياسات سجلي المسامية النيوترونية والكثافة خلال نطاقات Upper Safa Member أن الهيدروكربونات المتواجدة ستكون بشكل أساسي زيت بينما Lower Safa Member يظهر أن الهيدروكربونات المتواجدة به ستكون بشكل أساسي غاز. تم تفسير التوزيع الجانبي للهيدروكربونات المتواجدة من خلال عدد من الخرائط البارامترية المتساوية. حيث تُظهر تلك الخرائط تأثير بعض الخصائص البتروفيزيائية الهامة مثل المسامية الكلية، والمسامية الفعالة، وتشبع المياه لخزانات Upper & Lower Safa Members وتكمل هذه الخرائط البارامترية صورة تواجد الهيدروكربونات وتحديد مناطق تراكمها. كما تُظهر تلك الخرائط التباين الجانبي لهذه الخواص البتروفيزيائية التي قد تكون بسبب عدم التجانس الجانبي الظاهر، حيث تتغير الظاهرة من مكان إلى آخر دون اتجاه ثابت أو بسبب التراكيب المعقدة التي تؤثر على منطقة الدراسة أو كليهما. خريطة توزيع تشبع المياه لخزان Upper Safa Member تُظهر انخفاضاً في قيم تشبع المياه كلما نتجه نحو الاتجاه الشمالي الغربي من منطقة الدراسة مما يشير إلى أن حجم الهيدروكربون يزيد في هذا الاتجاه. بينما تُظهر خريطة توزيع تشبع المياه لخزان Lower Safa Member انخفاضاً في قيم تشبع المياه مع الاتجاه الشمالي لمنطقة الدراسة مما يشير إلى أن حجم الهيدروكربون يزيد في هذا الاتجاه نحو Well-1.

**ABSTRACT:** The Upper and Lower Safa reservoirs have become a very important exploration target in the Obaiyed field and have helped to improve exploration in the northwestern part of the Western Desert in Egypt. Therefore, the main purpose of this work is the evaluation of reservoir characteristics using the available well logging data and core data analysis in the Obaiyed field. The analysis revealed the average values of the petrophysical parameters of the studied zones. The integrated data has been used to support the exploration and development in the future field planning by doing more explorations in both the northwestern direction (where has more hydrocarbon bulk volume at the Upper Safa Member and has the highest formation pressure values) and the southwestern direction (where has more hydrocarbon bulk volume at the Lower Safa Member and has the highest formation pressure values) of the study area. The neutron-density log response through the zones of Upper Safa Member shows that the expected hydrocarbons will be mainly oil while the zones of Lower Safa Member show that the expected hydrocarbons will be mainly gas.

### 1. INTRODUCTION

Obaiyed Field is located in the Western Desert about 300 kilometers west of Alexandria, 70 kilometers south of the city of Mersa Matrouh, some 50 km south of the Mediterranean coast. The available well log data for the present study are wireline logs which include caliper, gamma-ray, resistivity, neutron, density, sonic logs, core and pressure data with a started depth of Masajid Formation (@ 2800 Measured Depth) for all five wells and Lower Safa structure map shows the locations of the wells (Figure 1).

The area is under discussion and exploration which produces hydrocarbons from the Upper and Lower Safa Members of Khatatba Formation in the

Middle Jurassic period. The main target of this study is studying the different reservoir parameters characterizing the pay zone utilizing well log data and the possibility of developing subsurface reservoirs of Upper Safa and Lower Safa Members that two of the four Members constituting the middle Jurassic Khatatba Formation and located in Shushan basin. The Upper Safa Member is underlain and overlain by the shelf carbonates of Kabrit and (Khatatba) Zahra Members, respectively. The Lower Safa Member is underlain and overlain by the Shifah Formation and shelf carbonates of Kabrit Members, respectively (Abu El Naga, M., 1984) (Figure 2).

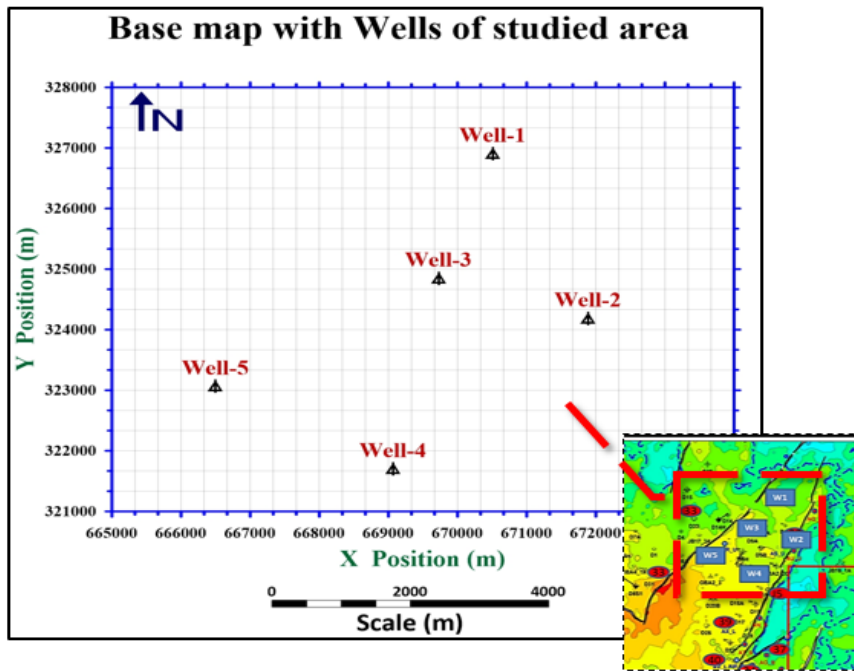


Figure 1: Base map with Wells of the studied area.

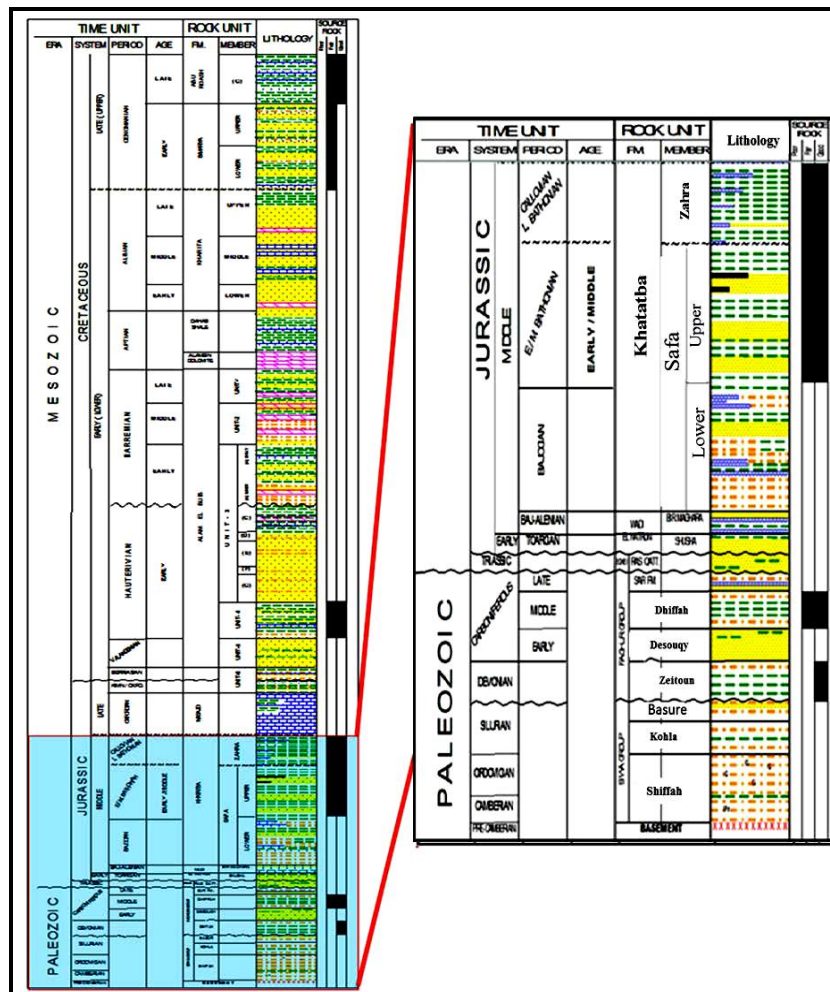


Figure 2: Generalized stratigraphic column of the North Western Desert, (after Khalda, 2001).

## Methodology

### Technique selection and preparation

Well-logging analysis is still the most important task after drilling which used to evaluate the reservoir parameters such as porosity, water, and hydrocarbon saturation, etc., Well-logging is one of the most successful methods nowadays used on every exploration and development well as a part of normal drilling practice. Science working on developing new well-logging and interpretation techniques to provide more information and greater accuracy of formations evaluation and detection of hydrocarbons. Well-logs deliver the data necessary for quantitative evaluation of hydrocarbons and water saturation, porosity, permeability, and the reservoir lithology.

### Determination of shale content

Shale volumes have been determined using gamma-ray, resistivity, and neutron-density, neutron-sonic and sonic-density methods for Upper & Lower Safa Members at Well-1 based on several equations that established by Schlumberger principles (1970), Pupon and Leveaux, (1971), and Schlumberger essentials (1972). The calculated shale volume of the Upper & Lower Safa Members shows that the gamma-ray method gives the minimum values of the shale volumes than that calculated from other methods.

### Determination of formation porosity

Available core data of well-1 are used to estimate

the most accurate porosity values of all determined porosities from the measurements from one, or a combination of sonic, density and neutron logs in the clean and shaly zones based on several equations that established by Wyllie et al. (1958), Schlumberger (1989), and Schlumberger (2015). Total and effective porosities have been determined using density, sonic, neutron-sonic and neutron-density methods for Upper & Lower Safa Members at Well-1. The calculated total and effective porosity of the Upper & Lower Safa Members compared with its core porosity data shows that the neutron-density method gives the most accurate values of the total porosity than that calculated by the other methods.

### Determination of the Formation Water Resistivity

The Pickett cross-plot (Pickett, 1972) is one of the simplest and most effective cross-plot methods. This technique only gives estimates of water saturation, determines formation water resistivity ( $R_w$ ) and cementation factor ( $m$ ). A knowledge of porosity is required, but the values of  $m$ ,  $R_w$ , and  $S_w$  can be obtained (Figure 3).

Estimated formation water resistivity of the Upper Safa Member in all studied wells (Well-1, Well-2, Well-3, Well-4, and Well-5) was 0.15 Ohm.m with  $m=1.9$  (Figure 4), while estimated formation water resistivity of the Lower Safa Member in all studied wells (Well-1, Well-2, Well-3, Well-4, and Well-5) was 0.05 Ohm.m with  $m=1.9$  (Figure 5).

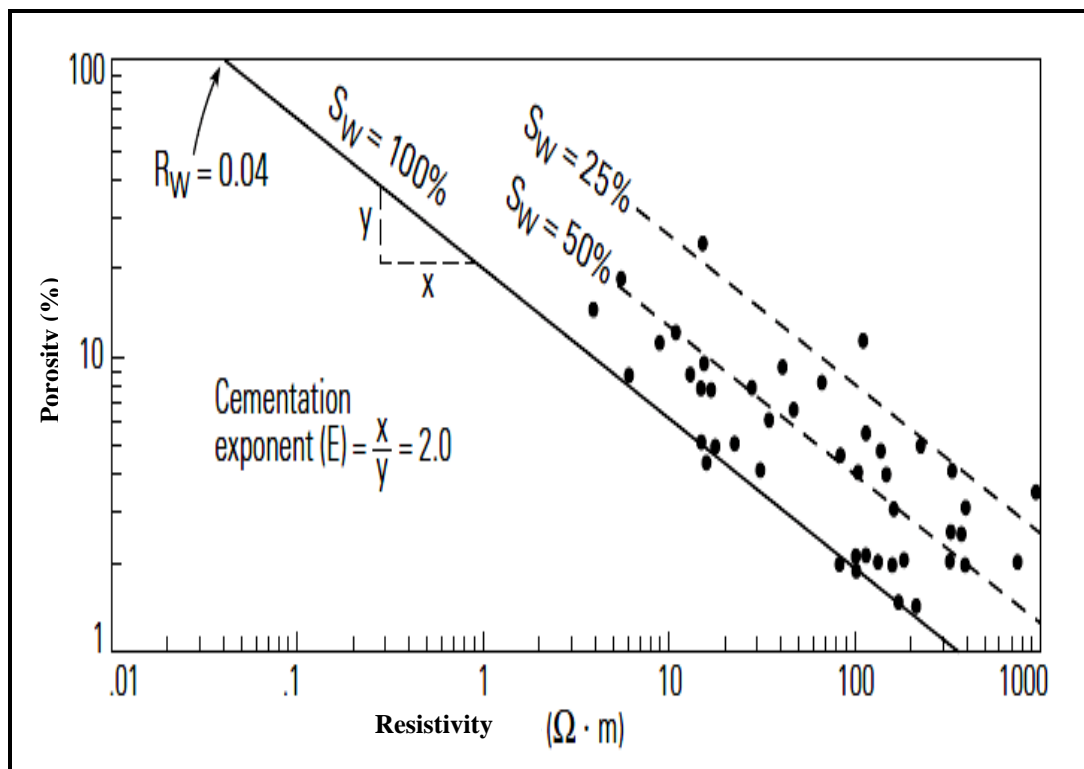


Figure 3: Example of Pickett Plot - porosity function of resistivity – where  $R_w=0.4$  when slope of 100%  $S_w$  line,  $m = 2$ .

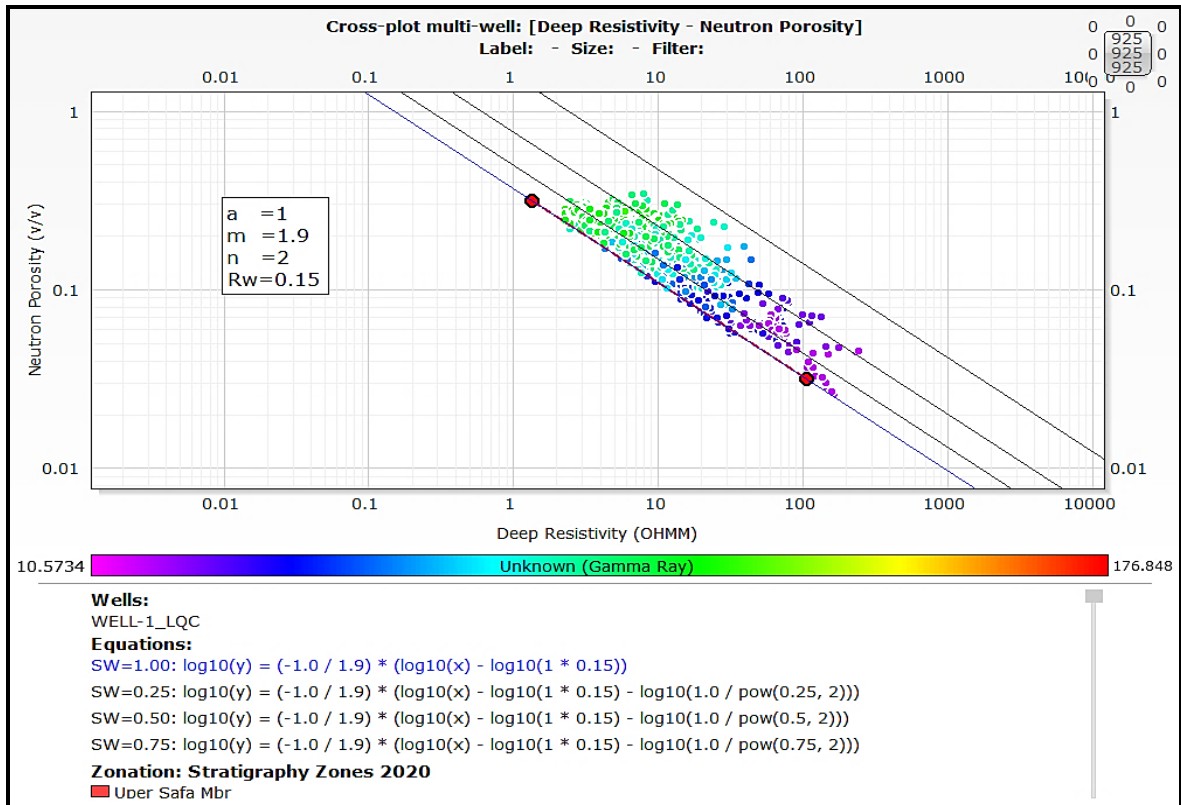


Figure 4: Pickett's plot for Upper Safa Member - Well-1.

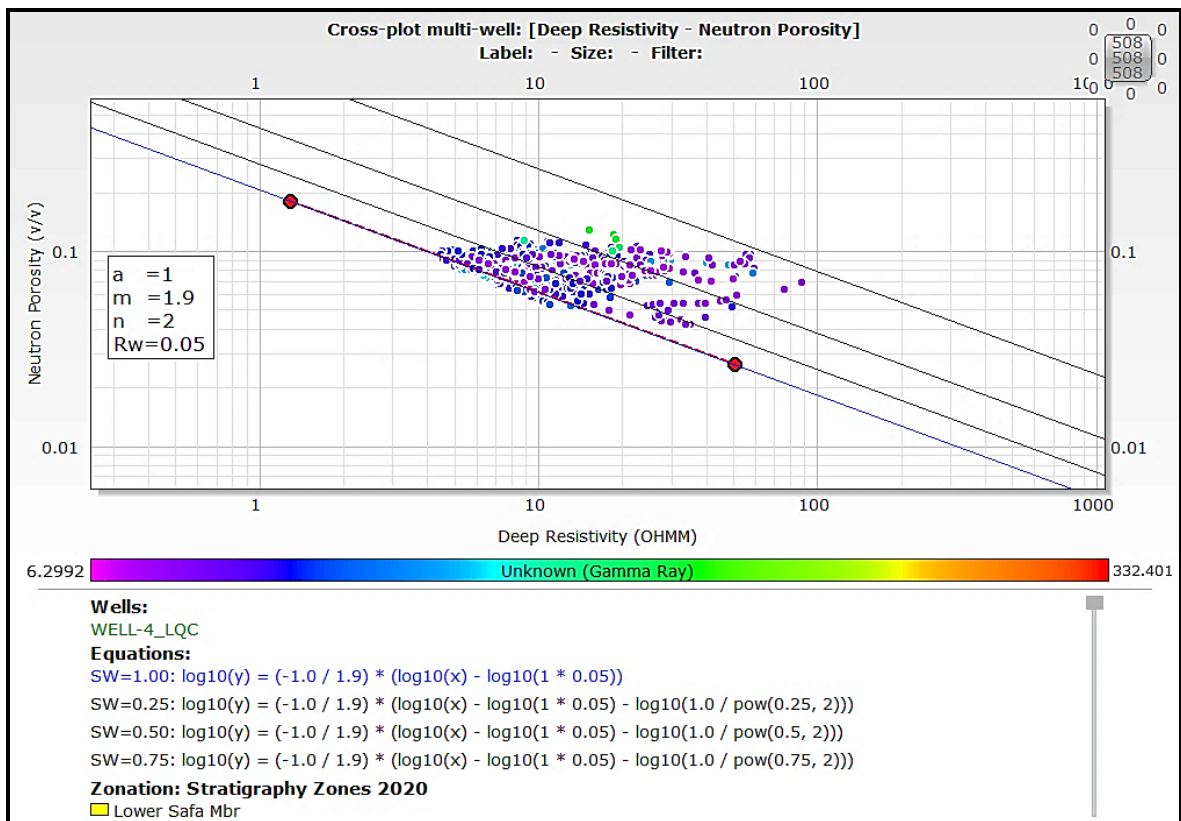


Figure 5: Pickett's plot for Lower Safa Member - Well-4.

**Determination of Formation Fluid Saturation**

The water saturation ( $S_w$ ) in the uninvaded zone is calculated through Archie's equation (Archie, C.E., 1942) in clean zones, while in shaly zones as in the case of this study for more accurate water saturation determination, we use both Dual water and Indonesia methods based on equations that established by Levenberg, Kenneth (1944), and Marquardt, Donald (1963). Then the Effective Bulk Volume of Water (BVWE) calculated from multiplying the water saturation in the calculated effective formation porosity.

Hydrocarbon saturation ( $S_h$ ) and water saturation ( $S_w$ ) represent the total saturated fluids of formation which equal to unity, then the Effective Bulk Volume of Hydrocarbon (BVHE) calculated from multiplying the hydrocarbon saturation in the calculated effective formation porosity.

**Lithology Identification**

The lithology identification model has been estimated from neutron-density cross plots (Figures 6&8), photoelectric-density cross plots (Figures 7 & 9),

and the simultaneous equations which were used in the ELAN-Plus computer program at Tech-log software to identify the stratigraphy and lithology of the Upper and Lower Safa reservoirs and the volume of each one. The formation components describe the minerals, rocks, and fluids likely to be encountered in appreciable quantity and provide the geological description of the types of formations to which the model applies. The primary answer sought from the ELAN-Plus application will be the volumes of certain formation components at each data level. Formation components exist in three groups: minerals, rocks, and fluids. The user must specify the components for which the program is to solve, by selecting them in the Process Editor which have been estimated depending on the geological history of the studied area and lithology identification by both neutron-density and photoelectric-density cross-plots which were identified previously as shale, sandstone and limestone for the Upper Safa Member, and sandstone and shale for the Lower Safa Member (Schlumberger, 2015).

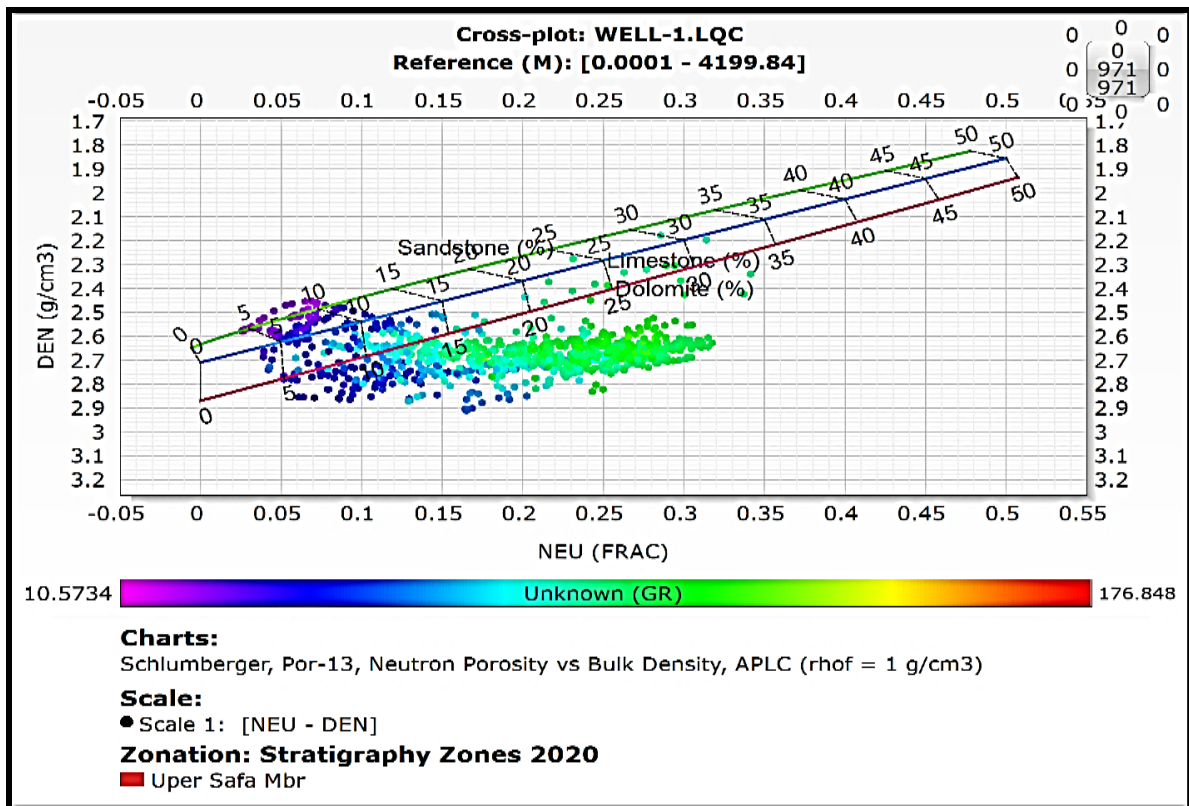


Figure 6: Neutron-Density Cross-plot for Upper Safa Member - Well-1.

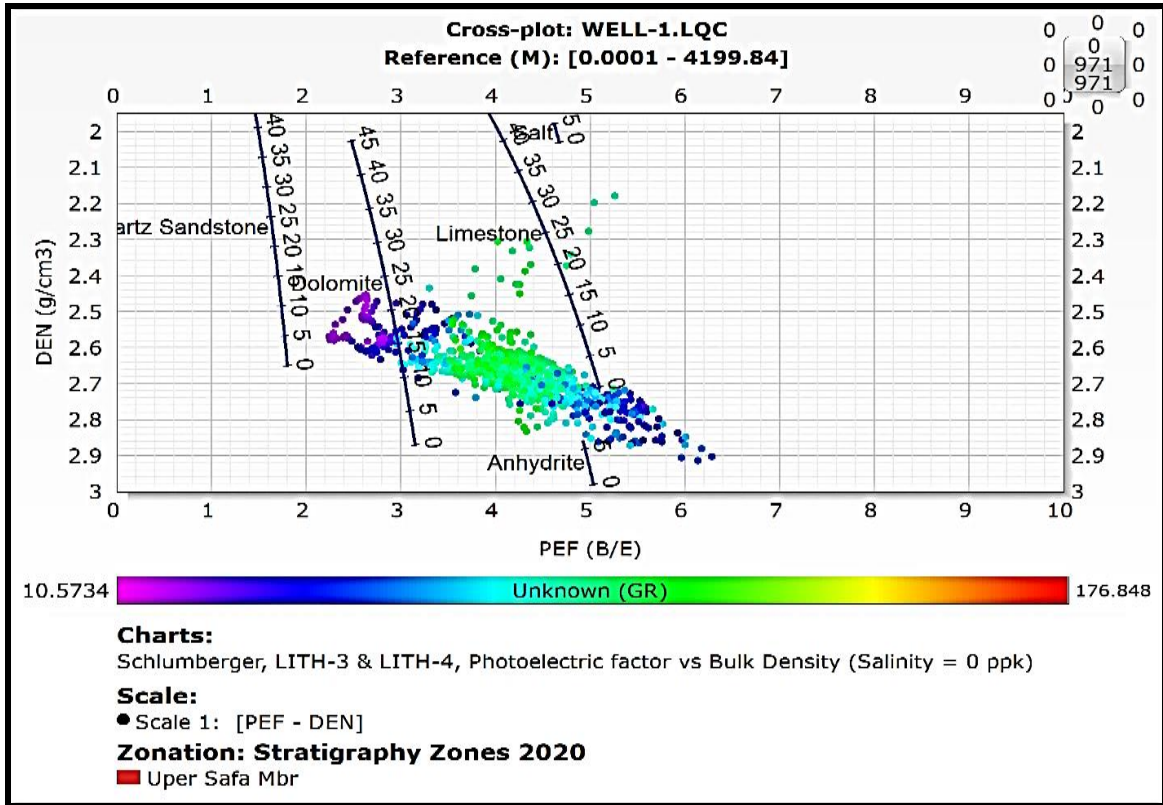


Figure 7: Photoelectric-Density Cross-plot for Upper Safa Member - Well-1.

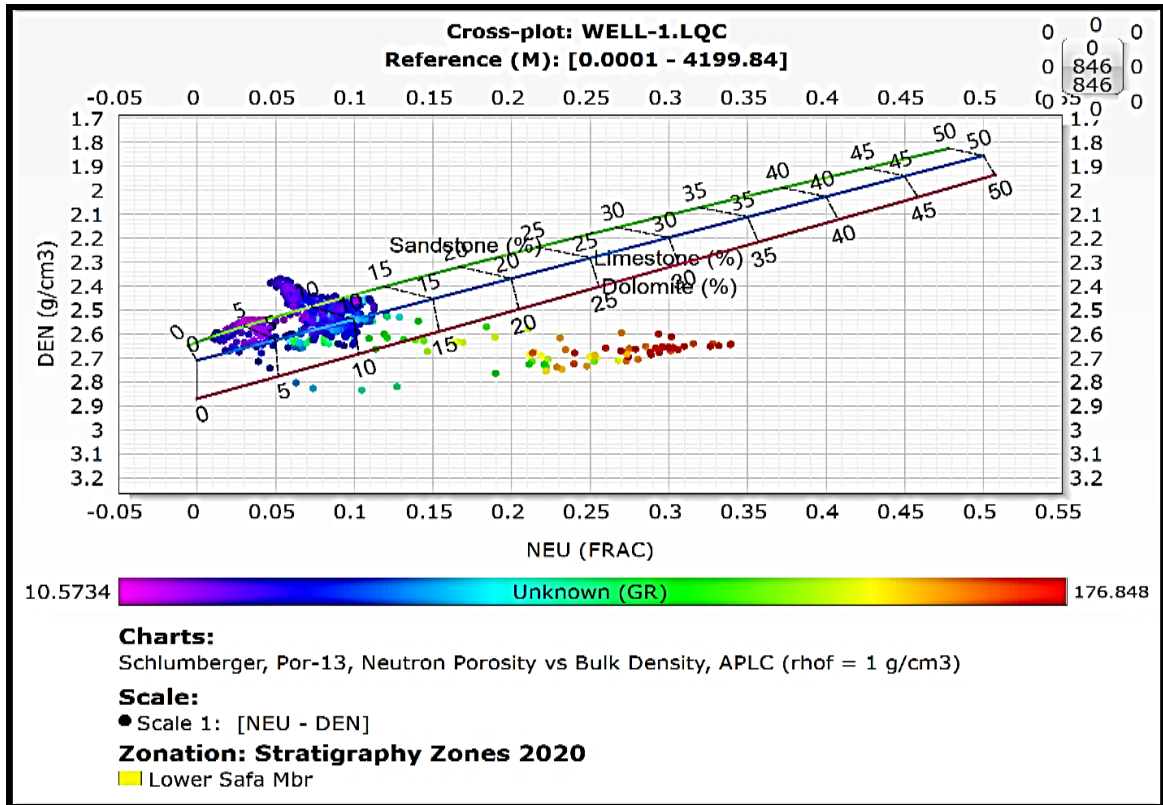


Figure 8: Neutron-Density Cross-plot for Lower Safa Member - Well-1.

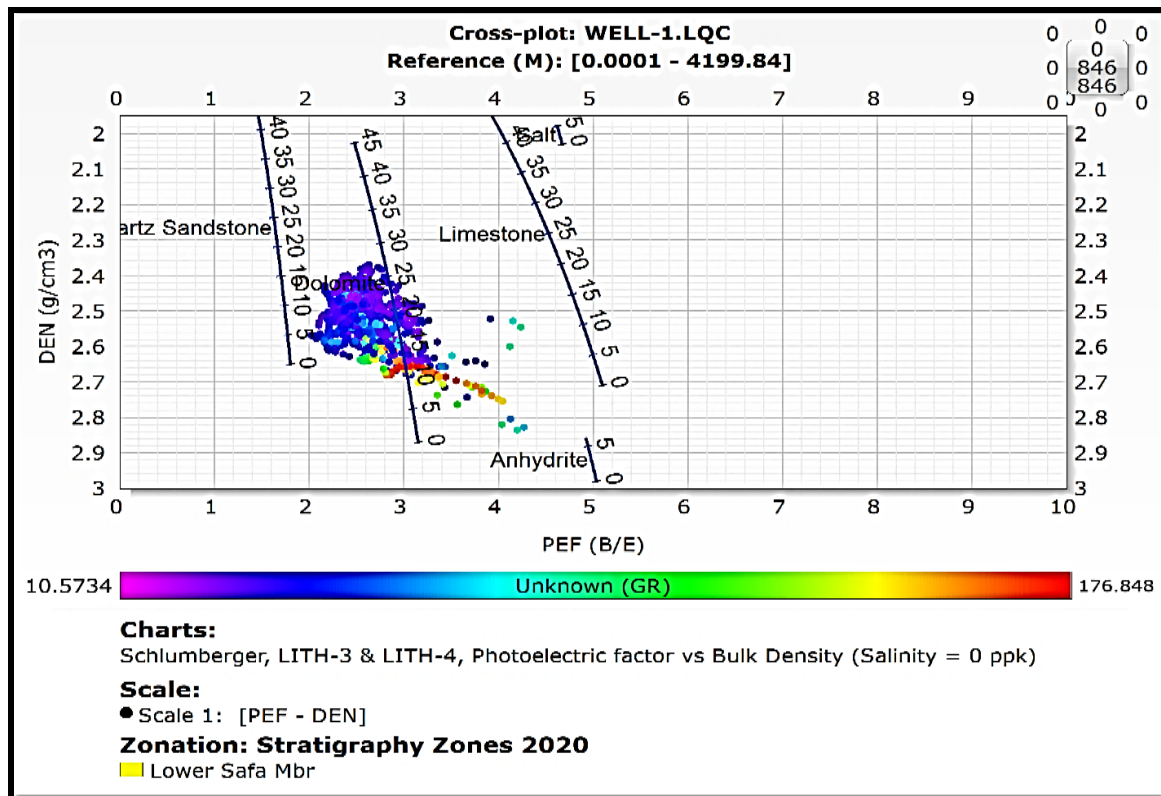


Figure 9: Photoelectric-Density Cross-plot for Lower Safa Member - Well-1.

## RESULTS AND DISCUSSION

Both the Upper Safa reservoir (in the interval 3553.33– 3757.05 m total vertical depth subsea) and the Lower Safa reservoir (in the interval 3723.47- 3936.72 m total vertical depth subsea) have shown several hydrocarbon pay zones.

- The lithological identification of the Upper Safa Member shows a majority of slightly calcareous to calcareous shale with streaks of slightly calcareous sandstone and argillaceous limestone. The Upper Safa reservoir have total net pay thickness range from 4.72 to 17.22 m with total porosity range from 6.75 to 8.84 % that is very close to its core porosity data and has been largely affected with the shale volume that ranged from 9.52 to 18.88 % and has resulted in relatively small effective porosity ranged from 4.27 to 5.81 %, and relatively high water saturation ranged from 43.72 to 70.11 %. Consequently, the hydrocarbon saturation is relatively small with a range from 29.89 to 56.28 %, and the effective bulk volume of hydrocarbon (BVHE) about 2.41%. (An example in Figure 10).
- The lithological identification of the Lower Safa Member shows a majority of sandstone with streaks of shale. The Lower Safa reservoir have net pay thickness range from 42.37 to 81.53 m with total porosity range from 7.83 to 11.44 % that is very close to its core porosity data and has been little affected with the shale volume that ranged from 6.07 to 14.08 % and has resulted in relatively good effective porosity ranged from 6.56 to 8.52 %, and relatively low water saturation ranged from 32.97 to 47.84 %. Consequently, the hydrocarbon saturation is relatively high with a range from 52.16 to 67.03 %, and the effective bulk volume of hydrocarbon (BVHE) about 4.99% (An example in Figure 11).
- The weighted average determined petrophysical properties for the reservoir of Upper Safa Member in the studied wells which have been calculated is shown in the following table (Table 1), and for the reservoir of Lower Safa Member (Table 2).

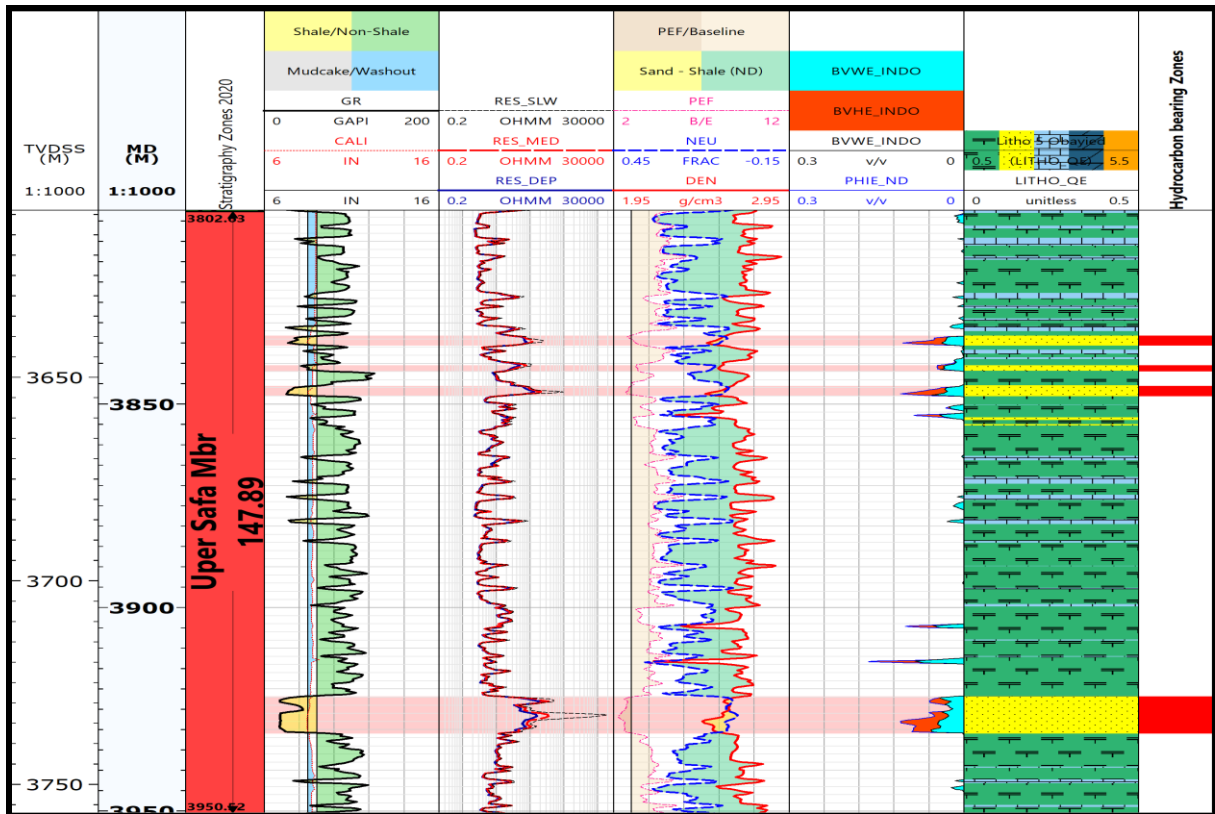


Figure 10: Litho-Saturation Cross-plot for Upper Safa Member - Well-1.

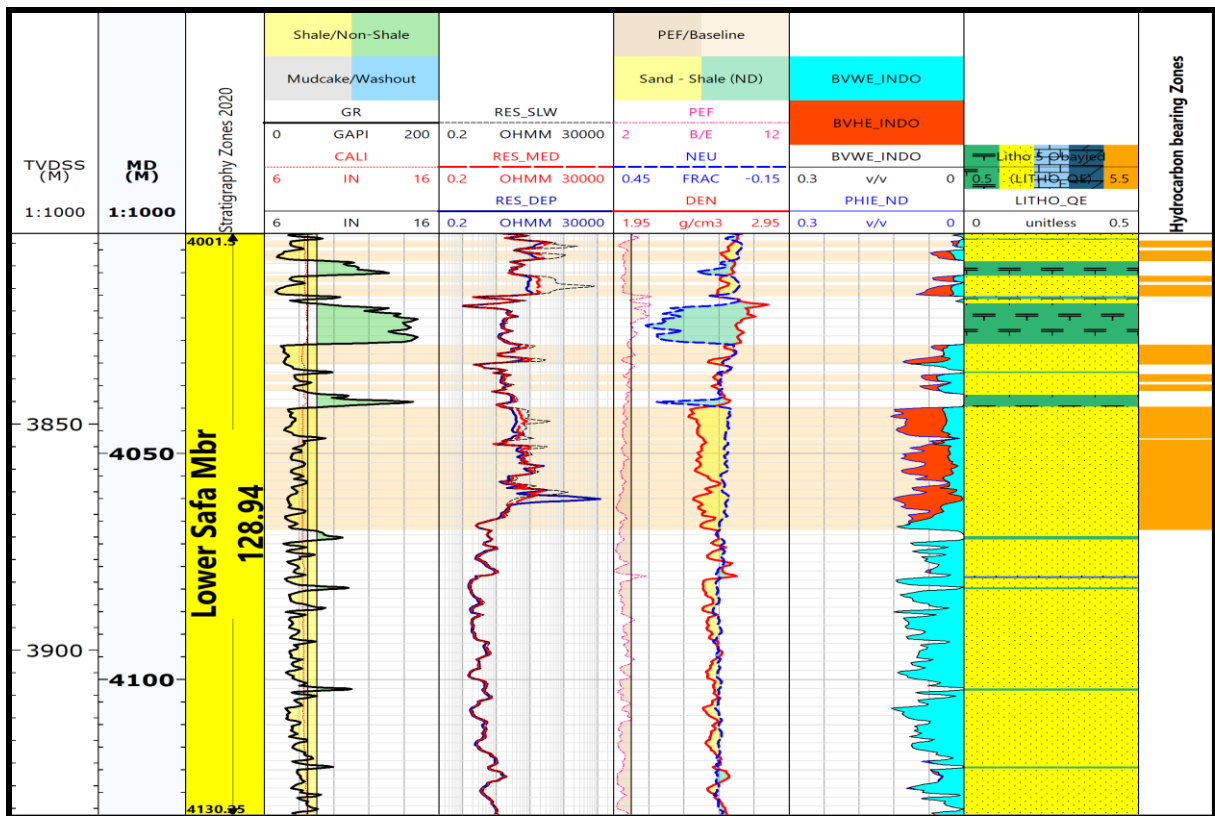


Figure 11: Litho-Saturation Cross-plot for Lower Safa Member - Well-1.



**Table 1: Petrophysical parameters of the reservoir of Upper Safa Member**

| Well   | Well Name    | Depth to Top TVDSS (m) | Depth to Bottom TVDSS (m) | Gross Thickness (m) | Net Pay Thickness (m) | V <sub>sh</sub> (%) | Ø <sub>t</sub> (%) | Ø <sub>e</sub> (%) | S <sub>w</sub> (%) | S <sub>h</sub> (%) |
|--------|--------------|------------------------|---------------------------|---------------------|-----------------------|---------------------|--------------------|--------------------|--------------------|--------------------|
| Well-1 | D13          | 3609.24                | 3757.05                   | 147.81              | 15.70                 | 9.52                | 7.80               | 5.81               | 65.28              | 34.72              |
| Well-2 | OBA D-30     | 3615.19                | 3744.48                   | 129.29              | 7.98                  | 10.19               | 7.07               | 4.98               | 66.37              | 33.63              |
| Well-3 | Obyd D21 ST1 | 3597.57                | 3754.85                   | 157.28              | 13.87                 | 13.06               | 7.15               | 4.39               | 43.72              | 56.28              |
| Well-4 | Obyd D3      | 3587.73                | 3708.73                   | 121.01              | 4.72                  | 18.88               | 8.84               | 4.87               | 70.11              | 29.89              |
| Well-5 | Obyd 2-3     | 3553.34                | 3664.51                   | 111.17              | 17.22                 | 11.69               | 6.75               | 4.27               | 47.92              | 52.08              |

**Table 2: Petrophysical parameters of the reservoir of Lower Safa Member**

| Well   | Well Name    | Depth to Top TVDSS (m) | Depth to Bottom TVDSS (m) | Gross Thickness (m) | Net Pay Thickness (m) | V <sub>sh</sub> (%) | Ø <sub>t</sub> (%) | Ø <sub>e</sub> (%) | S <sub>w</sub> (%) | S <sub>h</sub> (%) |
|--------|--------------|------------------------|---------------------------|---------------------|-----------------------|---------------------|--------------------|--------------------|--------------------|--------------------|
| Well-1 | D13          | 3807.82                | 3936.73                   | 128.91              | 42.37                 | 9.36                | 9.40               | 7.42               | 47.84              | 52.16              |
| Well-2 | OBA D-30     | 3786.87                | 3925.02                   | 138.15              | 73.19                 | 6.07                | 7.83               | 6.56               | 38.29              | 61.71              |
| Well-3 | Obyd D21 ST1 | 3779.02                | 3862.00                   | 82.98               | 53.49                 | 14.06               | 11.44              | 8.52               | 39.11              | 60.89              |
| Well-4 | Obyd D3      | 3747.65                | 3874.36                   | 126.71              | 68.38                 | 14.08               | 10.49              | 7.50               | 32.97              | 67.03              |
| Well-5 | Obyd 2-3     | 3723.48                | 3843.73                   | 120.26              | 81.53                 | 13.37               | 9.28               | 6.58               | 34.01              | 65.99              |

**Effective Porosity Distribution Map**

Based on the effective porosity ( $\phi_e$ ) estimated from combined Neutron-Density logs of all studied wells (Well-1, Well-2, Well-3, Well-4, and Well-5) we can establish the effective porosity distribution map for the reservoir of Upper Safa Member that shows the variation in porosity along the reservoir from 4.27% in the western direction at Well-5 and increasing toward the other wells in the southern direction at Well-4, the middle and the eastern direction at Well-3 and Well-2, respectively and the northern direction at Well-1 with the highest  $\phi_e$  value 5.81%, as shown in (Figure 12).

The effective porosity distribution map for the reservoir of Lower Safa Member was established. It shows a variation in porosity along the reservoir from 8.52% in the middle part at Well-3, then it is decreasing as going toward the west direction in Well-5, the south direction in Well-4, the north direction in Well-1, and the east direction in Well-2 with the lowest  $\phi_e$  value 6.56%, as shown in (Figure 13).

**Water Saturation Distribution Map**

Based on the effective water saturation ( $S_{we}$ ) calculated by the Indonesia method of all studied wells (Well-1, Well-2, Well-3, Well-4, and Well-5) we can establish the water saturation distribution map for the reservoir of Upper Safa Member that shows a variation in water saturation along the reservoir from 43.72% in the middle part at Well-3, then it is increasing as going toward the other wells in the southwestern direction at Well-5, the eastern direction at Well-2, the northern direction at Well-1, and the southern direction at Well-4 with the highest  $S_{we}$  value 70.12% (Figure 14).

The water saturation distribution map for the reservoir of Lower Safa Member shows a variation in water saturation along the reservoir from 32.97% in the southern part at Well-4, then it is increasing as going toward the other wells in the southwestern direction at Well-5, the eastern direction at Well-2, the middle direction at Well-3, and the northern direction at Well-1 with the highest  $S_{we}$  value 47.84% (Figure 15).

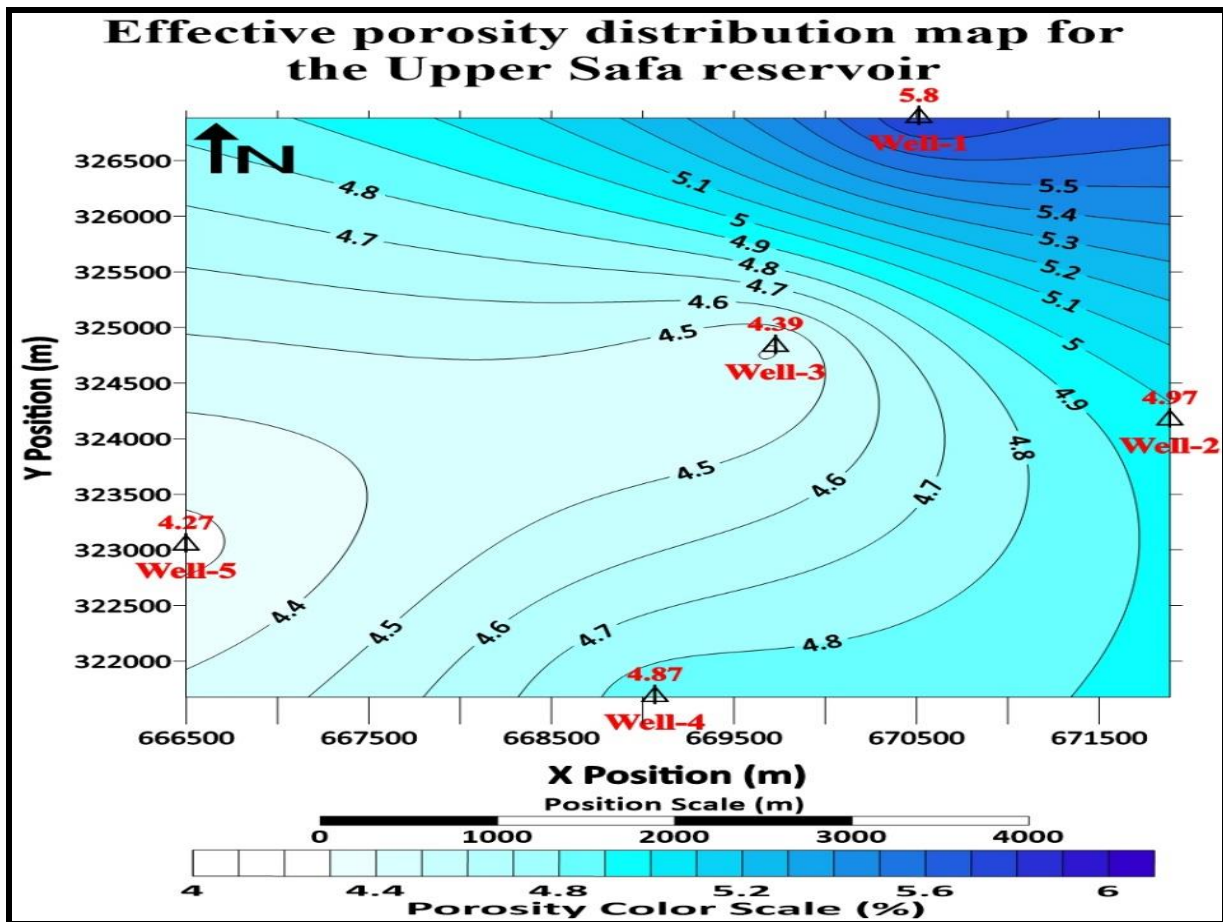


Figure 12: Effective porosity distribution map for reservoir of Upper Safa Member in Obayied field.

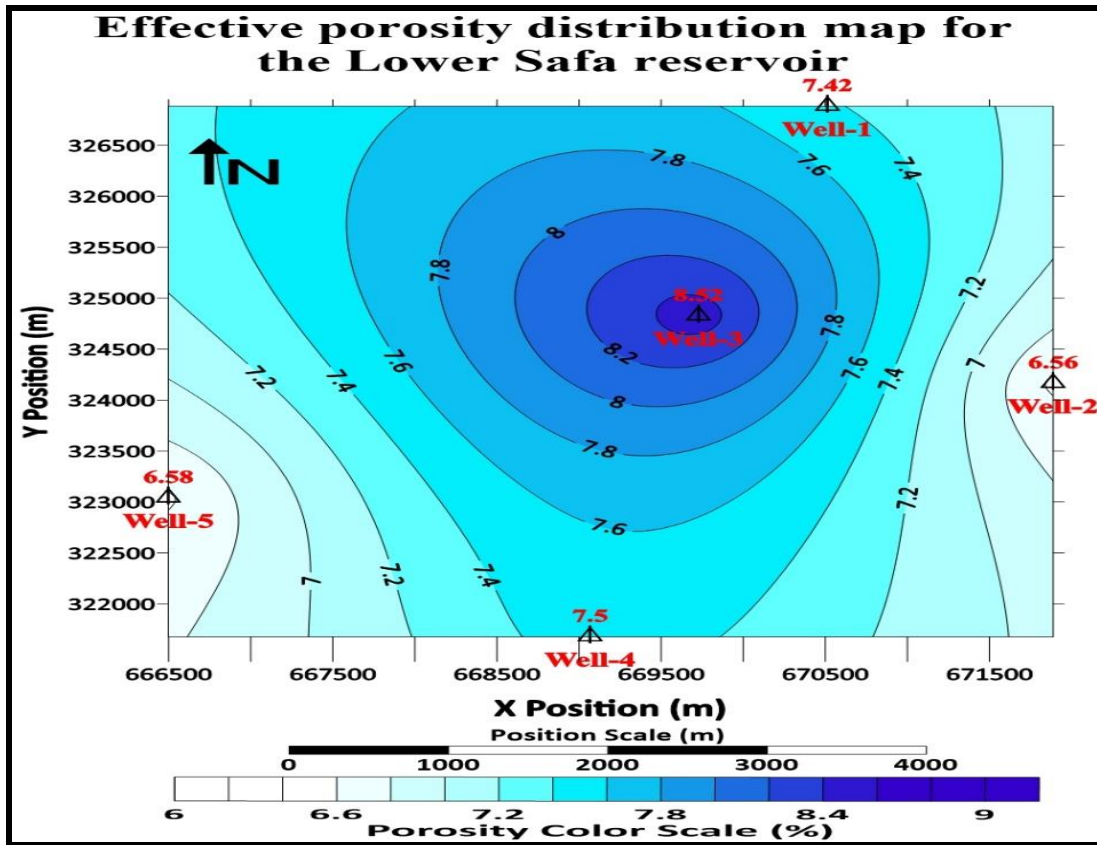


Figure 13: Effective porosity distribution map for reservoir of Lower Safa Member in Obayied field.

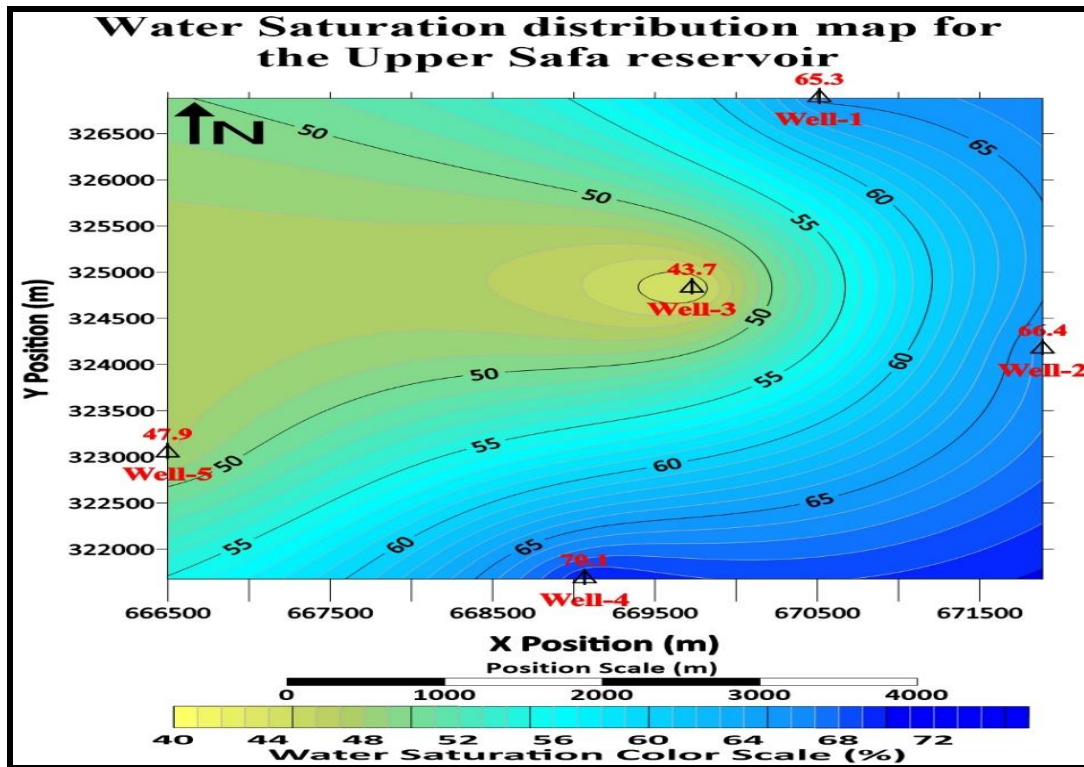


Figure 14: Water saturation distribution map for Upper Safa reservoir in Obayied field.

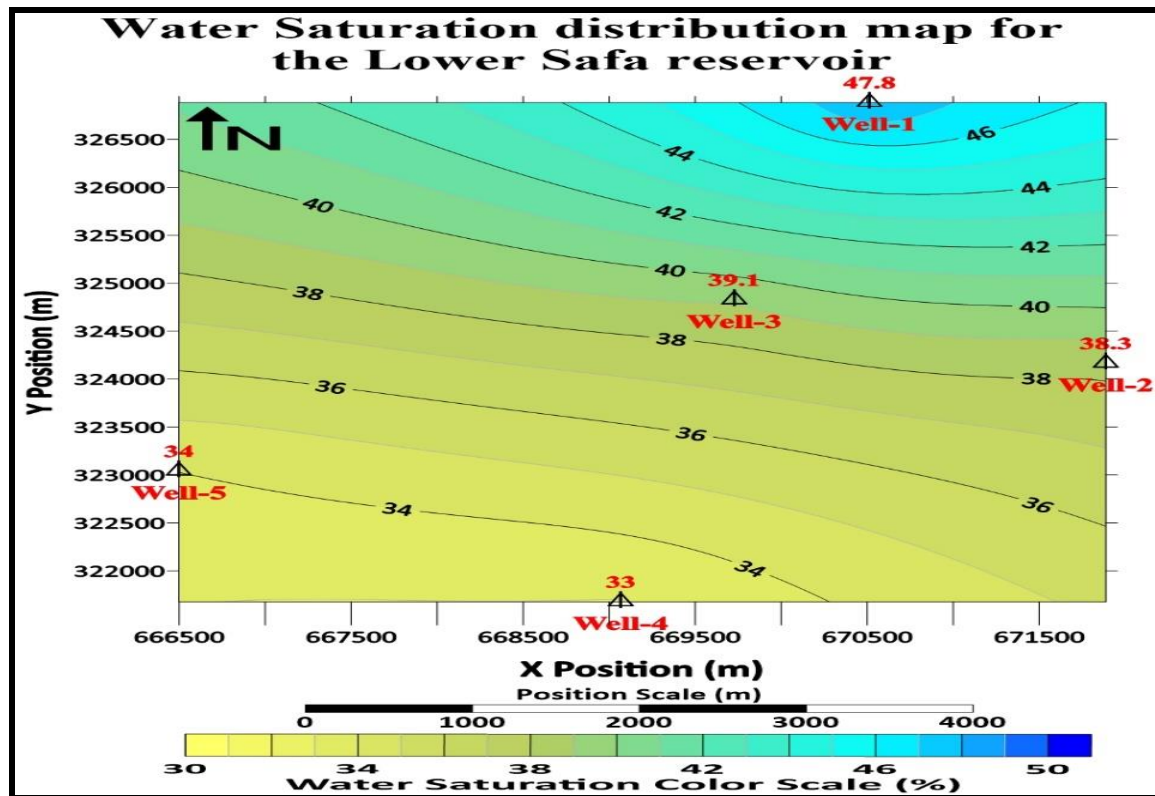


Figure 15: Water saturation distribution map for Lower Safa reservoir in Obaiyed field.

## CONCLUSIONS

The different well logging data of five wells and core porosity data of wells (Well-1, Well-4, and Well-5) in the Obaiyed field were used to study the different petrophysical parameters of the reservoirs of Upper and Lower Safa Members.

The average values of the petrophysical parameters of these zones have been estimated. The nature of the fluids in the permeable pay zones is determined by the analysis of the porosity and resistivity logs. The interpretation of the response of the resistivity tools in hydrocarbon and water-bearing zones relies on an understanding of the changes in resistivities that occur in the region close to the Wellbore of a permeable zone. The neutron-density log response through the zones of Upper Safa Member show that the hydrocarbons will be mainly oil while the zones of Lower Safa Member show that the hydrocarbons will be mainly gas.

The lateral distribution of hydrocarbon occurrences has been explained through several iso-parametric maps. These maps show the effect of some important petrophysical parameters such as the total porosity, the effective porosity, and the water saturation for Upper and Lower Safa reservoirs. These iso-parametric maps complete the picture of hydrocarbon

potentiality and delineating the areas for hydrocarbon accumulation. These maps illuminate the lateral variation of these petrophysical parameters which may be due to the lateral facies heterogeneity, where facies change from place to place without consistent trend or due to the complex structure affecting the study area or both of them.

The water saturation distribution map for the reservoir of Upper Safa Member shows decreasing in water saturation values as going toward the northwestern direction of the study area which indicates that more hydrocarbon bulk volume in this direction and has the highest formation pressure values.

The water saturation distribution map for the reservoir of Lower Safa Member shows decreasing in water saturation values as going toward the northern direction of the study area which indicates that more hydrocarbon bulk volumes in this direction at Well-1 that has high formation pressure values while also Well-4 in the southern direction of the study area has the highest formation pressure values.

## Acknowledgments

The authors are deeply indebted to Badr Petroleum Company for providing the data used in this study.

**REFERENCES**

- Abu El Naga, M. (1984):** Paleozoic and Mesozoic depocenters and hydrocarbon generating areas, north Western Desert. EGPC 7<sup>th</sup> Petroleum Exploration Seminar, Cairo. p. 269- 287.
- Archie, C.E. (1942):** The electrical resistivity logs as an aid in determining some reservoir characteristics. Transactions of the AIME, Vol.146, p. 54-62.
- Khalda Petroleum Company Internal Report (2001):** Paleontological Studies for Qasr Field.
- Levenberg, Kenneth (1944):** A Method for the Solution of Certain Non-Linear Problems in Least Squares. Quarterly of Applied Mathematics. p. 164-168.
- Marquardt, Donald (1963):** An Algorithm for Least-Squares Estimation of Nonlinear Parameters. SIAM Journal on Applied Mathematics. p. 431-441.
- Pickett, G.R. (1972):** Practical formation evaluation. Golden Colorado. G. R. Pickett, Inc., p.160.
- Poupon, A. and Leveaux, J. (1971):** Evaluation of Water Saturation in Shaly Formations. The Log Analyst, p.1-2.
- Schlumberger (1970):** Well evaluation. conf., Libya. Serv. Tech. Schlumberger, France, p.96.
- Schlumberger (1972):** The essentials of log interpretation practice. Schlumberger Ltd., France, p. 45-67.
- Schlumberger (1989):** Log interpretation Principles/ Applications. Schlumberger Well Services, Inc. p.225.
- Schlumberger (2015):** Techlog Online Help 2015.3 in Guru 2015.4 software for in-context support guidance and training, Schlumberger Information Solutions (SIS), Inc., pages of petrophysics.
- Wyllie, M.R.J., Gregory, A.R., Gardner, G.H.F. (1958):** An Experimental Investigation of Factors Affecting Elastic Wave Velocities in Porous Media, Geophysics, Vol.23, No.3, p. 459-493.

